Environmental Science and Pollution Research (2022) 29:43758–43769
https://doi.org/10.1007/s11356-020-12244-3

RESEARCH ARTICLE

Concrete slump prediction modeling with a fine-tuned convolutional neural network: hybridizing sea lion and dragonfly algorithms

Kumar Shaswat [1]

Received: 22 May 2020 / Accepted: 25 December 2020 / Published online: 22 January 2021

Abstract

High-strength concrete (HSC) is defined as concrete that meets a special combination of uniformity and performance requirements, which cannot be attained routinely via traditional constituents and normal mixing, placing, and curing procedures. It is a complex material since modeling its behavior is a difficult task. This paper intends to show the feasible applicability of optimized convolutional neural networks (CNN) for predicting the slump in HSC. The following are the parameters that given as the input for the prediction of slump: cement (kg/m^3), slag (kg/m^3), fly ash (kg/m^3), water (kg/m^3), super-plasticizer (kg/m^3), coarse aggregate (kg/m^3), and fine aggregate (kg/m^3). In order to make the prediction more accurate, the design of CNN is assisted with optimization logic by making some fine-tuned filter size of the convolutional layer. For this optimization purpose, this work presents a new "hybrid" algorithm that incorporates the concept of sea lion optimization algorithm (SLnO) and dragonfly algorithm (DA) and is named as Levy updated-sea lion optimization algorithm (LU-SLnO). Finally, the performance of the proposed work is compared and proved over the state-of-the-art models with respect to error measure and convergence analysis.

Keywords High-strength concrete · Slump · Workability · Optimized CNN · Optimization

Abbreviations

ANN	Artificial neural network
BPC	Bentonite plastic concrete
M5Tree	M5 model tree
UEO	Used engine oil
GA	Genetic algorithm
RMC	Ready mix concrete
BPNN	Backpropagation neural network
GEP	Gene expression programming
HPC	High-performance concrete
PCE	Polycarboxylate ether
RMSE	Root mean square error
SF	Silica fume
AASC	Alkali-activated slag concretes
HSC	High-strength concrete
SCC	Self-compacting concrete
ELM	Extreme learning machines
MARS	Multivariate adaptive regression splines
MAPE	Mean absolute percentage error
MAD	Mean absolute deviation

Responsible Editor: Philippe Garrigues

✉ Kumar Shaswat
er.kumar.shaswat@gmail.com

[1] Department of Civil Engineering, Bennett University, Greater Noida, Uttar Pradesh 201310, India

Introduction

Concrete (Prasad et al. 2020; Vieira and Figueiredo 2020;Kaufmann 2020;Honglei et al. 2020) is defined as the core building material that deployed all around the world. It is highly noted for its durability, abrasion resistance, resistance to fire, high compressive strength, and impermeability. It is very much essential to compact the concrete for contributing the maximum structured strength. The concrete quality that satisfies the aforesaid need is explained as workability. It is a parameter that defines the concrete property, which identifies the effort needed for compaction, placing, and finishing with reduced homogeneity loss. The overall work required to initialize and maintain flow aids in the determination of the effort needed to place a concrete mixture. On the one hand, this mainly relies on the lubricant's rheological property (the cement paste) and the internal friction amongst the aggregate

particles, in contrast to the friction among the surface and concrete of the model.

The concrete workability (Sokhansefat et al. 2019;Abdalla et al. 2019;Fang et al. 2018;Li et al. 2018) typically relies on numerous factors and one of them is the water-cement ratio, which greatly affects the workability. The workability and water-cement ratio factor are directly proportional to each other. So, the maximization in the water-cement ratio maximizes the concrete workability as well. The test that is used to calculate the parameters nearer to workability is termed the slump test (Domone 1998;Yuan et al. 2020; Tay et al. 2019;Lu et al. 2015) and further offers helpful information on this workability. The concrete consistency is commonly measured by this method and it is deployed mostly on the sites or labs. The drop in the peak of the slumped fresh concrete is measured to deduce the slump from this test. Additional information regarding the concrete workability might be gained by analyzing the slump shape in concrete.

Each construction type needs concrete testing for identifying the slump obtained from the fresh concrete to assure the concrete with needed strength and workability, though no much research works have existed in the literature work with respect to slump prediction of concrete. The purpose of the supply chain in the cement industry is to propose the right supply chain for cement and to prove that the supply chain can produce value for cement companies (Taghipour et al. 2013; Vosooghidizaji et al. 2020; Agudelo and Isabel 2009). The researchers still look at the parameter characterization, which impacts the concrete's slump value. Furthermore, the technical personnel has tried on various mixture proportions for gaining the concrete of suitable and desired workability, but it results in material wastage and cost and is time-consuming. Therefore, machine learning models (Nilsen et al. 2019; Feng et al. 2020; Bayar and Bilir 2019; Rousseau et al. 2019; Zheng et al. 2019; (Yu et al. 2018) (Yu et al. 2019; Nguyen et al. 2019; Nguyen et al. 2020) (Beno et al. 2014) need to be developed for the sake of minimizing the design cost and saving time and can be the better option for predicting the concrete slump. CNN is more efficient than traditional classifiers, because it reduces the number of parameters to be given as input for learning. It uses pooling and convolution operations thereby perform parameter sharing and so it can perform the learning with a limited number of attributes. This makes the CNN to work on any device. Though it has several advantages than other deep learning algorithms, it is not much used in literary works.

The major contribution of this work is stated below:

- This work introduces a new fine-tuned CNN design for predicting the slump of concrete, which is done by the logic of optimization.
- Presents a novel hybrid concept named LU-SLnO, which is the hybrid version of sea lion and dragonfly models.
- The proposed work in the view of performance is compared and proved over other classical works with respect to error and convergence analysis.

The paper organization is as follows: The "Literature survey" section defines the literature survey on review papers under the topic slump prediction in concrete. The "Designing of optimization-assisted deep learning for slump prediction" section elucidates the designing of optimization-assisted deep learning for slump prediction. The "Proposed hybrid algorithm: objective function and solution encoding" section describes the proposed hybrid algorithm with objective function and solution encoding. The "Results and discussions" section manifests the results along with their discussions. Finally, concludes the paper in the "Conclusions" section.

Literature survey

Related works

Amlashi et al. (2019) have introduced prediction models for predicting the strength of elastic modulus, slump, and cubic samples of BPC. In this, soft computing models like M5Tree, ANN, and MARS were deployed and differentiated. Furthermore, the analysis was made regarding the parameters as well. The experimental analysis thus validated the improved performance of the ANN method over other comparative methods with the precise prediction of these parameters. The slump of BPC gets impacted more by the water variables and less by sand variables.

Shafiq et al. (2018) have presented the investigational outcomes in response to the impact of UEO on hardened concrete and slump properties. For this investigation, the preparation of three concrete groups has been made. A control mix along with the mix of 0.15% UEO dosage was composed within every group. From this, it can say that the small dosage of UEO has increased the reasonable slump amount in concrete by calculating the slump measurement of fresh concrete. Typically, the result has confirmed that there was a substantial minimization in oxygen porosity coefficient and permeability of entire concrete mixes using the small dosage of used engine oil, whereby termed as the pointer of improved long-term durability.

Chandwani et al. (2015) have exposed the work of combining two different nature-inspired computational intelligence approaches like ANN and GA to model the RMC slump. This was exploited using the design mix constituents such as water-binder ratio, cement, coarse aggregates, sand, fly ash, and admixture. Under six diverse statistical parameters, the hybrid model (ANN-GA) was scrutinized in terms of performance over the BPNN model. From this study, the prediction accuracy and convergence speed of ANN seem to get improved using hybridized ANN and GA. The concrete slump was predicted using this trained hybrid approach. This does not need any usage of multiple trials with diverse design mix proportions.

Chen et al. (2014) have processed several parallel subpopulations for avoiding the local optima and also for improving

the search diversity at the instance of the GEP optimization process. Through the whole subpopulations, the fascinating solutions were rapidly distributed by the hyper-cubic topology. The case learning thus revealed that the parallel hyper-cubic GEP needs to be more precise than the fundamental GEP and the other two regression methods for evaluating the HPC slump flow. In this, the implemented model was highly preferred since it provides clear formulas with measurable parameters, even though both the implemented model and BPNN provides similar performance.

Meng et al. (2019) have investigated the impact of slump-retaining PCE dispersant, SF, and their mixture, over the hardened and fresh properties of normal Portland cement paste. The properties used for investigation were rheological properties, hydration kinetics, compressive strength, and setting time. The resultant outcomes have formulated, in which the cement hydration rates were accelerated and initial/final setting time was reduced by SF. To the end, there established a feasible correlation among rheological properties, hydration kinetics, and compressive strength evolution. This in turns offered a fundamental to optimize binder formulation and proportion of high/ultra-large performance concrete.

Bondar et al. (2018) have highlighted the investigational findings of AASC for offering an inclusive view on the impact of design variables mixture related to strength, slump, and chloride binding and transport. The result thus verified that AASC has been modeled for diverse grades and diverse workability of concrete. The diffusivity outcomes have formulated that the excess addition of water has not managed the pore connectivity/structure in AASC. Hence, the designing of AASC was made on the basis of the water/binder ratio required for a particular mechanical performance. Furthermore, it was observed that there was an increase in the chloride binding capacity along with the raise in the silica content of the activator and/or the paste content of the concrete.

Agrawal and Sharma (2010) have intended to demonstrate the probable application of NN for slump prediction in HSC. Based on the existing test data having 349 diverse concrete mix designs of HSC collected from a specific RMC batching plant, the NN was trained, tested, and modeled. The prediction of the slump in concrete was made using the most flexible NN model. The input parameters utilized in this dataset were fly ash, cement, coarse aggregate (10 mm), sand, water, water/binder ratio, and super-plasticizer. The experimental outcomes were differentiated based on the performance function or error function.

Ma et al. (2017) have introduced an enhanced mix design approach of SCC in correspondence to the correlation between average diameter of coarse aggregate, slump flow, and coarse aggregate volume. Similarly, in the volume of coarse aggregate condition, the small SF was made suitable by large coarse aggregate average diameter; still, the small coarse aggregate average diameter had matched large SF. The investigational outcomes have thus demonstrated that the SCC properties involving compressive strength and workability have satisfied the requirements. This enhanced mix design model aided in advancing SCC and cuts the cost in real-world engineering projects with better results.

Review

Table 1 shows the features and challenges of the conventional methods regarding concrete slump prediction. ANN is the used method in (Amlashi et al. 2019) that attains minimum values for RMSE, MAD, and MAPE parameters with the reduced slump, compressive strength, and elastic modulus, even though sensitivity analysis is needed to conduct for future use and recommends incorporating the global optimization bio-inspired algorithms. Modified Darcy's equation (Shafiq et al. 2018) achieves high performance and has reasonable minimization in total porosity. But, there is no concern on UEO effect on the long-term durability of concrete. ANN-GA (Chandwani et al. 2015) has better robustness with fast convergence to the global optimum and poses a better prediction of slump value, even though we plan to use the ELMs to model the material behavior of concrete and the overall performance needs to be improved further. Parallel hyper-cubic GEP (Chen et al. 2014) achieves lower RMSE error and has better accuracy in estimating the slump flow of HPC. But, the prediction ability is restricted because of high non-linear problems. The Bingham fluid model (Meng et al. 2019) has enhanced cement hydration kinetics and has reduced plastic viscosity and yield stress. However, it poses fewer hydration enhancements and the difference in strength between plain and binary pastes is significantly smaller. Fick's second law of diffusion (Bondar et al. 2018) produces AASC of required strength and poses better workability. Yet, further study is needed to discern the binding capacity. ANN (Agrawal and Sharma 2010) is convenient and easier in predicting any mix proportions and has a better estimation of slump prediction. It still needs further studies for the slump prediction using some soft computing techniques. Improved mix design method (Ma et al. 2017) has excellent workability and low cost and is very useful in developing SCC. For future work, more attention is needed on SCC workability.

Designing of optimization-assisted deep learning for slump prediction

This paper plans to develop a novel machine learning model for predicting the slump in HSC. The block diagram of the

Table 1 Features and challenges of conventional concrete slump prediction models

Author (citation)	Methodology	Features	Challenges
Amlashi et al. (2019)	ANN	• Attains minimum values for RMSE, MAD, and MAPE parameters • Reduced slump, compressive strength, and elastic modules	• Sensitivity analysis is needed to conduct for future use • Recommends to incorporate the global optimization bio-inspired algorithms
Shafiq et al. (2018)	Modified Darcy's Equation	• Achieves high performance • Reasonable minimization in total porosity	• No concern on UEO effect on the long-term durability of concrete
Chandwani et al. (2015)	ANN-GA	• Better robustness • Fast convergence to global optimum • Better prediction of slump value	• Will plan to use the ELMs to model the material behavior of concrete • Overall performance needs to be improved further
Chen et al. (2014)	Parallel hyper-cubic GEP	• Achieves lower RMSE error • Better accuracy in estimating the slump flow of HPC	• Prediction ability is restricted because of high non-linear problems
Meng et al. (2019)	Bingham fluid model	• Enhanced cement hydration kinetics • Reduced plastic viscosity and yield stress	• Less hydration enhancements • The difference in strength between plain and binary pastes is significantly smaller
Bondar et al. (2018)	Fick's second law of diffusion	• Produce AASC of required strength • Better workability	• Further study is needed to discern the binding capacity
Agrawal and Sharma (2010)	ANN	• Convenient and easier in predicting any mix proportions • Better estimation of slump prediction	• Further studies needed for the slump prediction using some soft computing techniques
Ma et al. (2017)	Improved mix design method	• Excellent workability and low cost • Useful in developing SCC	• More attention is needed in the future on SCC workability

concrete slump prediction modelis depicted in Fig. 1. From the literature work, most of the prediction model relies with the application of the ANN model. This research work makes an attempt to design a new optimized CNN for predicting the slump, which is trained with the input data patterns. They are cement (kg/m^3), super-plasticizer (kg/m^3), slag (kg/m^3), fly ash (kg/m^3), water (kg/m^3), coarse aggregate (kg/m^3), and fine aggregate (kg/m^3). Furthermore, the synthetic data are as well generated with the above data. Moreover, the fine-tuning of filter size in the convolutional layer makes the model more accurate and precise in predicting the slump. For this optimization purpose, this work introduces a new "hybrid" algorithm termed LU-SLnO.

Design of fine-tuned convolutional neural network

Even after applying the computer vision tasks within the NNs, the prior knowledge integration within the network architecture is a crucial one for superior generalization performance. The spatial information practice is the main intention of CNN O'Shea and Nash (2015) and hence, it relies on discrete convolution.

Convolutional layer The convolutional layers have to use small filters *fs* (e.g., 3 × 3 to the maximum as 5 × 5), based on a stride of $S = 1$ and, significantly, padding the input volume with zeros whereby the convolutional layer has not changed the input's spatial dimensions. In this work, the filter size *fs* is optimally tuned using the proposed LU-SLnO algorithm.

Let the convolutional layer is assumed as *cl*. Consequently, the input of the layer *cl* consists of $p_1^{(cl-1)}$ feature maps from the earlier layers, each of size $p_2^{(cl-1)} \times p_3^{(cl-1)}$. While $cl = 1$, the input remains as the single data *cl* that is the composition

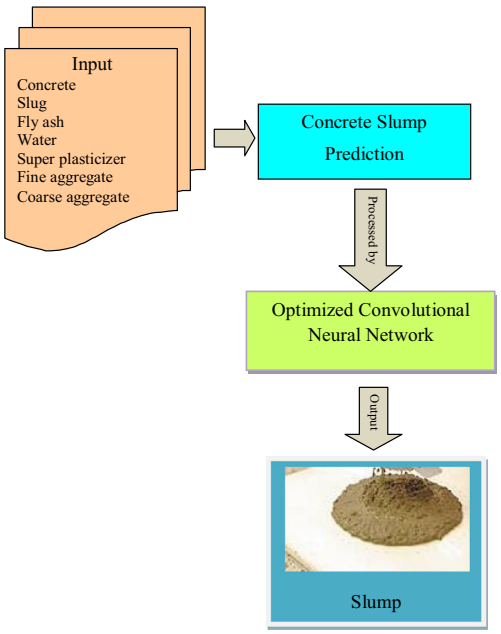

Fig. 1 Block diagram of the concrete slump prediction model

of one or more channels, which in turn accept the raw data as input of CNN. The layer cl poses the output that contains p_1^{cl} feature maps of size $p_2^{cl} \times p_3^{cl}$. $\widehat{X}_i^{cl}$ delineates the ith feature map in layer cl and is formulated as per Eq. (1).

$$\widehat{X}_i^{cl} = D_i^{(cl)} + \sum_{j=1}^{p_1^{(cl-1)}} P_{i.j}^{(cl)} * \widehat{X}_j^{(cl-1)} \tag{1}$$

In which, bias matrix is expressed as $D_i^{(cl)}$ and the filter of size $2s_1^{cl}+1 \times 2s_2^{cl}+1$ linking the jth feature map in a layer $cl-1$ along with the feature map in cl is depicted by $P_{i.j}^{(cl)}$. The output feature map has provided the size as per Eq. (2).

$$p_2^{cl} = p_2^{(cl-1)} - 2s_1^{cl} \; and \; p_3^{cl} = p_3^{(cl-1)} - 2s_2^{cl} \tag{2}$$

Frequently, the filters are deployed for measuring the similarity of the fixed feature map $\widehat{X}_i^{cl}$, i.e., $P_{i.j}^{(cl)} = P_{i.k}^{(cl)} \; for \; j \neq k$. Every feature map $\widehat{X}_i^{cl}$ in the layer cl consists of $p_2^{cl}.p_3^{cl}$ units organized in two-dimensional array form. The output is calculated as per the unit at position (g, h) is portrayed in Eqs. (3) and (4).

$$\left(\widehat{X}_i^{cl}\right)_{g,h} = \left(D_i^{(cl)}\right)_{g,h} + \sum_{j=1}^{p_1^{(cl-1)}} \left(P_{i.j}^{(cl)} * \widehat{X}_j^{(cl-1)}\right)_{g,h} \tag{3}$$

$$= D_i^{(cl)}\Big)_{g,h} + \sum_{j=1}^{p_1^{(cl-1)}} \sum_{d=-s_1^{cl}}^{s_1^{cl}} \sum_{e=-s_2^{cl}}^{s_2^{cl}} \left(P_{i.j}^{(cl)}\right)_{d,e} \left(\widehat{X}_j^{(cl-1)}\right)_{g+d,,h+e} \tag{4}$$

In which, $\widehat{X}_j^{(cl-1)}$ is referred as the trainable weight of the network and the bias matrix is explicated as $D_i^{(cl)}$. The skipping factors u_1^{cl} and u_2^{cl} is evaluated by deploying subsampling. The fundamental notation is to fix the count of pixels in the vertical and horizontal direction, once before the filter application. The size of the output feature maps by employing the skipping factor is evaluated based on Eq. (5).

$$p_2^{cl} = \frac{p_2^{(cl-1)} - 2s_1^{cl}}{u_1^{cl}+1} \; and \; p_3^{cl} = \frac{p_3^{(cl-1)} - 2s_2^{cl}}{u_2^{cl}+1} \tag{5}$$

Non-linearity layer Let the layer cl is considered as a non-linearity layer, wherein the input is p_1^{cl} feature maps and the output included again with $p_1^{cl} = p_1^{(cl-1)}$ feature maps offered the size of each as $p_2^{(cl-1)} \times p_3^{(cl-1)}$, which is stated in Eq. (6).

$$\widehat{X}_i^{cl} = f\left(\widehat{X}_i^{(cl-1)}\right) \tag{6}$$

In which, the activation function in the layer cl is signified as f and works on pointwise. The supplementary gain coefficient is formulated using Eq. (7).

$$\widehat{X}_i^{cl} = ga_i f\left(\widehat{X}_i^{(cl-1)}\right) \tag{7}$$

Rectification Let the rectification layer be considered as cl. Each component has the absolute value with the feature maps and is evaluated based on Eq. (8) with the input comprised of $p_1^{(cl-1)}$ feature map having size $p_2^{(cl-1)} \times p_3^{(cl-1)}$.

$$\widehat{X}_i^{cl} = \left|\widehat{X}_i^{cl}\right| \tag{8}$$

In which, the absolute value is measured as pointwise so that the output contains the $p_1^{cl} = p_1^{(cl-1)}$ feature maps with no alteration in size.

Feature pooling and subsampling layer Considering cl as the pooling layer and their outputs is comprised of $p_1^{cl} = p_1^{(cl-1)}$ feature maps having minimized size. Typically, in every feature map, the pooling works by locating the windows at non-overlapping positions and sustains one value for every window, whereby the subsampling of feature maps is exploited. Two kinds of pooling are differentiated in this layer as follows:

Average pooling: The operation is exploited as average pooling when the boxcar filter is utilized and is demonstrated as Q_{Ag}.
Max pooling: The maximum value of every window is assumed to be in max pooling and is expressed using Q_{Max}.

Fully connected layer Let us assume the fully connected layer as cl. If the layer $cl-1$ is not considered as fully connected, then the layer cl gets the input other than $p_1^{(cl-1)}$ feature maps having the size $p_2^{(cl-1)} \times p_3^{(cl-1)}$ and the j layer with the ith unit is measured as per Eq. (9).

$$\widehat{x}_i^{cl} = f\left(v_i^{cl}\right) \; with \; v_i^{cl} = \sum_{j=1}^{p_1^{cl-1}} \sum_{g=1}^{p_2^{cl-1}} \sum_{h=1}^{p_3^{cl-1}} W_{i,j,g,h}^{cl} \left(\widehat{X}_j^{(cl-1)}\right) \tag{9}$$

In which, the weight that associates the unit at the position (g, h) in the jth feature map of layer $cl-1$ and the ith unit in cl is elucidated by $W_{i,j,g,h}^{cl}$. The block diagram of the optimized CNN model is depicted in Fig. 2.

Proposed hybrid algorithm: objective function and solution encoding

Solution encoding

As mentioned above, the filter size fs of the convolutional layer is optimally tuned using the proposed hybrid algorithm. The input given to the implemented work is elucidated in Fig. 3. The main objective defined in the implemented prediction model is given in

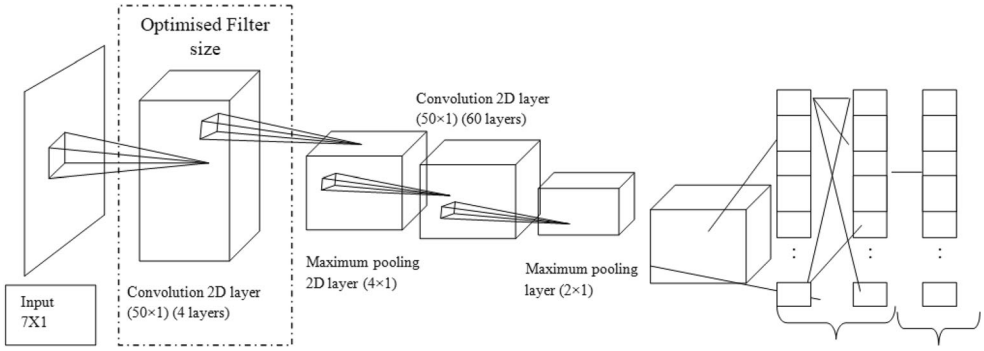

Fig. 2 Optimized CNN model

Eq. (10), where *err* is the error among the predicted and actual value.

$$obj = \min(err) \tag{10}$$

Proposed LU-SLnO algorithm

The proposed LU-SLnO algorithm merges the principle of DA in the sea lion model that obviously deals with the better convergence rate and speed. The proposed SLnO includes three major phases:

- Tracking and chasing of prey by their whiskers.
- Pursuing and encircling the prey by calling other members of their subgroups to join them.
- Attack the prey.

Mathematical modeling of the proposed algorithm is exploited with four stages that are termed as proposed tracking a detection phase, social hierarchy, attacking, and encircling prey.

Detecting and tracking phase The whiskers facilitate the sea lion to sense the existing prey and for detecting their position when the direction of whiskers is in the opposite of the water wave's direction, though the vibration of whiskers is less while its orientation is as same as the present orientation.

Sea lion positioned the prey's location and call for other members to merge its subgroup for pursuing and hunting the prey. The leader is the sea lion which calls others and the updating of the position of target prey is exploited by other members. This algorithm assumes the target prey as the closer one to the optimal solution or recent best solution. Towards the following iteration, to get closer, the sea lion moves over the target prey. In this scenario, the position of the sea lion gets updated using the arithmetical model of Levy update in DA (Jafari and Chaleshtari 2017) given in Eq. (11).

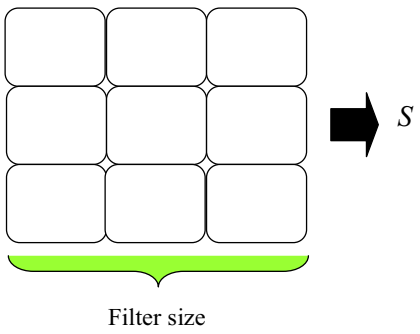

Fig. 3 Solution encoding

$$\overrightarrow{S}(t+1) = \overrightarrow{S}(t) + Levy(y) \times \overrightarrow{S}(t) \tag{11}$$

$$Levy(y) = 0.01 \times \frac{r_1 \times \Phi}{|r_2|^{\frac{1}{y}}} \tag{12}$$

$$\Phi = \left(\frac{\Gamma(1+\xi) \times \sin\frac{\pi\xi}{2}}{\Gamma\left(\frac{1+\xi}{2}\right) \times \xi \times 2^{\left(\frac{\xi-1}{2}\right)}} \right) \tag{13}$$

Vocalization phase Sea lions can adapt to stay in both land and water. The sound of sea lion in water can travel four times quicker than in the air. While chasing or hunting the prey, the communication of sea lions is made via numerous vocalizations. In addition, they have the capacity on detecting the sound both on and under the water. On identifying prey, the sea lion calls on other members for encircling and attacking the prey. This is arithmetically given in Eqs. (14), (15), and (16), where the speed of sea lion leader's sound is portrayed as $\overrightarrow{S_{leader}}$, the sounds speed in water and air is demonstrated as $\overrightarrow{P_1}$ and $\overrightarrow{P_2}$.

$$\overrightarrow{S_{leader}} = \left| \left(\overrightarrow{P_1} \left(1 + \overrightarrow{P_2} \right) \right) / \overrightarrow{P_2} \right| \tag{14}$$

$$\overrightarrow{P_1} = \sin\theta \tag{15}$$

$$\overrightarrow{P_2} = \sin\varphi \tag{16}$$

Attacking phase In the exploration part, the sea lions' hunting behavior is formulated based on two stages as follows:

a) Dwindling encircling approach: This approach is explicated based on Levy value (Nair and Muthuvel 2019) *K Levy*(*y*) in Eq. (11) and is decreased steadily via a course of iteration from 2 to 0. This reducing factor directs the sea lion to forward on and to encircle the prey.
b) Circle updating position: The bait ball of fishes is the prime target of sea lions and the attack is started from edges which is explicated as per Eq. (17), in which the distance among the search agent (sea lion) and best optimal solution (target prey) is represented as $\vec{M}(t)-\vec{S}(t)$, the absolute value is indicated by ||, and the random number is manifested as *l* and falls between − 1 and 1.

$$\vec{S}(t+1)=\left|\vec{M}(t)-\vec{S}(t).\cos(2\pi l)\right|+\vec{M}(t) \tag{17}$$

Prey searching From the best search agent in the exploration phase, the position update of the sea lion is formulated. The search agent's position update in the exploration phase is evaluated with respect to the chosen random sea lion. It can also say that the SLnO algorithm carries out a global search agent and determine the global optimum solution, while $\vec{F}$ is larger than 1. This is defined as in Eqs. (18) and (19). The flowchart of the proposed LU-SLnO algorithm is exploited in Fig. 4. The pseudo-code of the implemented LU-SLnO algorithm is given in Algorithm 1.

$$\overrightarrow{Dis}=\left|2\vec{B}.\overrightarrow{S_{rnd}}(t)-\vec{S}(t)\right| \tag{18}$$

$$\vec{S}(t+1)=\overrightarrow{S_{rnd}}(t)-\overrightarrow{Dis}.\vec{H} \tag{19}$$

Algorithm 1: Pseudocode of LU-SLnO Algorithm

```
Initialization of population
Choose S_rnd
Estimate the fitness function for every search agent
if (i < max iter)
estimate S_leader as per Eq. (14)
If( S_leader <0.25)
    If ( Levy(y) <1)
        Update the position of current search agent using the Levy update in DA algorithm given in Eq. (11)
    else
        Select a random search agent S_rnd
        Update the current search agent location using Eq. (19)
    End if
else
    Update the current search agent location using Eq. (17)
End if
If the search agent do not belong to any S_leader
    Go to the first if condition
else
    Compute the fitness function for every search agent
    Update S as per the better solution
    Return S , which is the best solution
End if
End if
stop
```

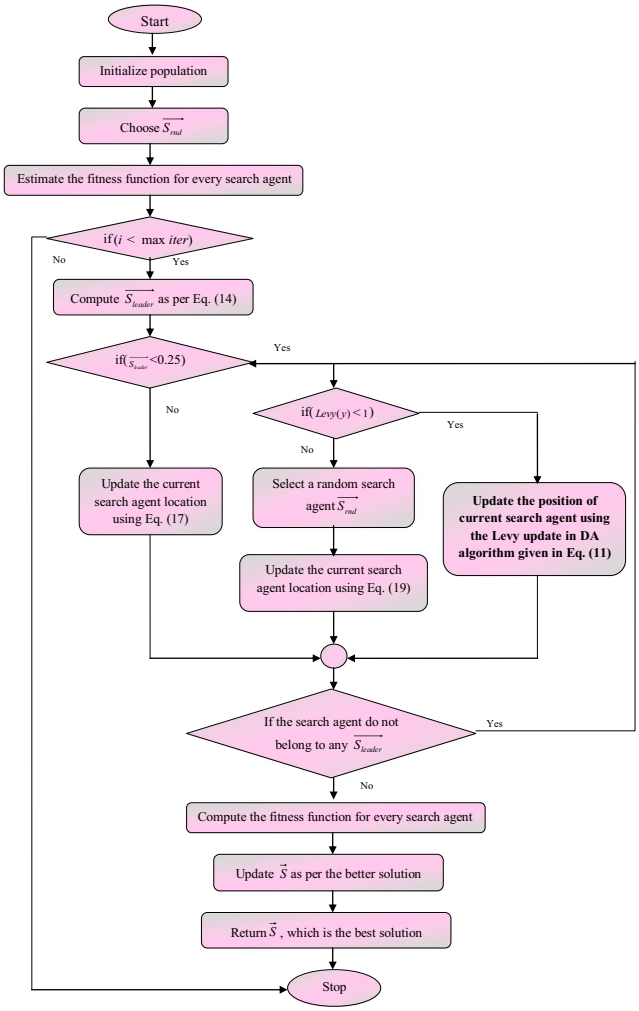

Fig. 4 Flowchart of the proposed LU-SLnO algorithm

Results and discussions

Simulation setup

The evaluation of this implemented slump prediction model is made using MATLAB. The dataset used for this experiment is downloaded from the link: https://archive.ics.uci.edu/ml/datasets/Concrete+Slump+Test. The data set includes 103 data samples. There are 7 input variables namely cement, slag, fly ash, water, SP, coarse aggregate, fine aggregate, and 3 output variables slump (cm), flow (cm), and 28-day compressive strength (Mpa). Since this paper intents to predict the slump, we have used the slump (cm) as the output variable. Super-plasticizer has an effect on workability and to collect the data; 78 mix proportions were performed at the first phase of the experiment. Furthermore, 35 more proportions are extended to acquire the total samples of 103. More details about the experiment can be referred from Yeh (2008), Yeh and I-Cheng (2009), Yeh and I-Cheng (2008), Yeh and I-Cheng (2007), and Yeh and I-Cheng (2006). The analysis in this work is exploited by varying the learning percentage to a different extent as 50, 60, 70, and 80. For example, with a learning rate of 60%, there are 62 data samples used for training and validation for the remaining 38 data samples were used for the testing set. Furthermore, the 62% of data samples are divided into 70% for training and 30% for testing. Hence, 43 out of the 62 data samples are used for training, while 18 data samples are used for validation The experimental analysis is made by comparing the proposed work with the conventional models like SLnO (Masadeh et al. 2019), DA (Jafari and Chaleshtari 2017; Jadhav and Gomathi 2019), LA (Boothalingam 2018; (Brammya and Deepa 2019), and LA-RE (Shaswat, personal communication) under actual and predicted values and convergence. Furthermore, the overall error analysis is as well as formulated under certain error measures like RMSE, MD, MASE, SMAPE, one norm, MAE, infinity norm, and two norms. The purpose of the slump prediction method is to minimize the error between actual and predicted value. The formula for some errors is given below.

$$MSE = \sum_{i=1}^{N} \frac{(Predicted_i - Actual_i)^2}{N}$$

$$RMSE = \sqrt{\sum_{i=1}^{N} \frac{(Predicted_i - Actual_i)^2}{N}}$$

$$MAE = \sqrt{\sum_{i=1}^{N} \frac{|Predicted_i - Actual|}{N}}$$

$$SMAPE = \frac{100}{N} \sum_{i=1}^{N} \frac{Predicted_i - Actual_i}{Predicted_i}$$

Analysis on actual vs. predicted slump

The analysis on actual versus the predicted slump of the implemented model against the classical models is exhibited in Fig. 5. These values are plotted for different learning percentages like 50, 60, 70, and 80 and the results are analyzed. From the graphical representation, it is monitored that the predicted value of the proposed model has highly got closer with the actual slump while comparing over other compared models. The prediction rate is high if the actual and the predicted values are the same. Hence, from this analysis, it is clear that the implemented approach has achieved a superior prediction rate than any other models.

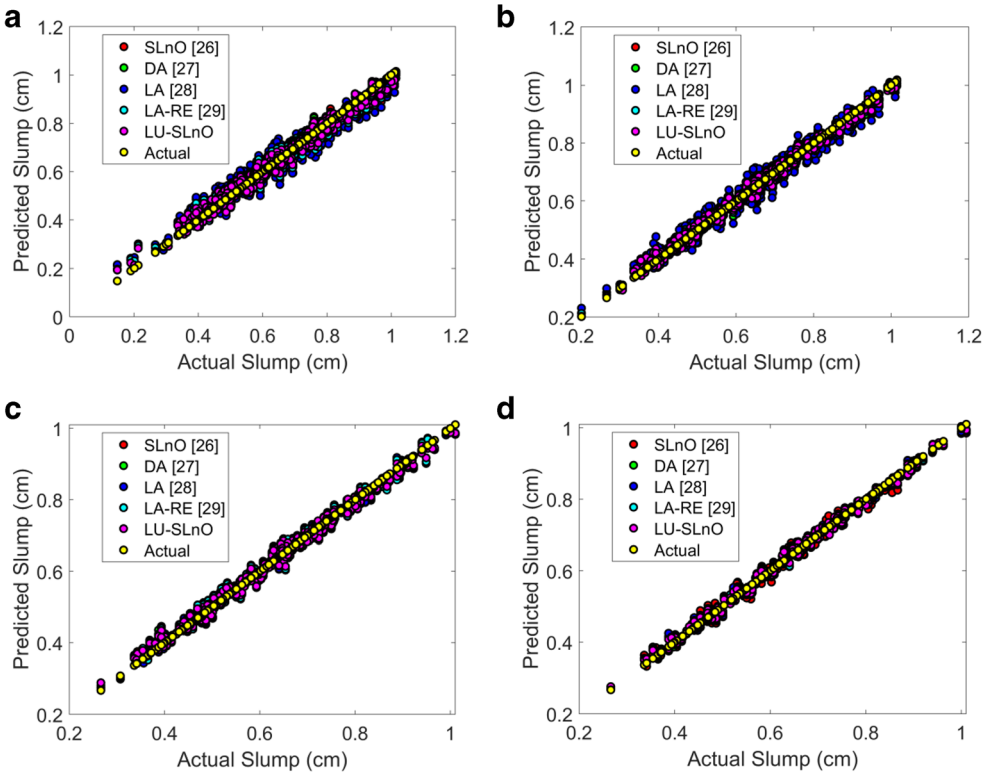

Fig. 5 On actual slump vs. predicted slump of the proposed model over state-of-the-art models for different learning percentage **a** 50, **b** 60, **c** 70, and **d** 80

Convergence analysis

Figure 6 illustrates the convergence analysis of the proposed model against other compared models under diverse learning percentages. The error performance needs to be minimum for attaining the best prediction performance. Particularly, while considering the results under 50% of learning, the error is at the maximum level for both the proposed and conventional

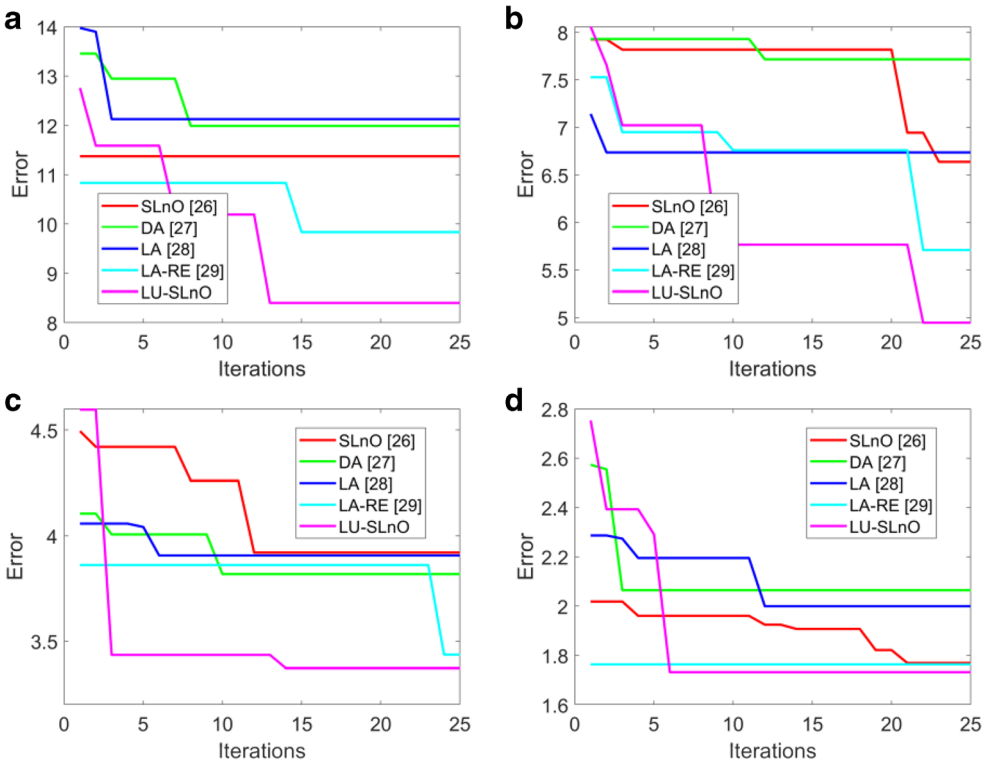

Fig. 6 Convergence analysis of the proposed model over state-of-the-art models for varied learning percentage **a** 50, **b** 60, **c** 70, and **d** 80

Table 2 Overall error analysis of the proposed model over conventional models

Learning percentage=50	MD	Infinity norm	MASE	One norm	MAE	Two norms	RMSE	SMAPE
SLnO (Masadeh et al. 2019)	4.6113	0.093085	0.15496	13.43	0.02686	0.74179	0.033174	0.045366
DA (Jafari and Chaleshtari 2017)	3.833	0.082326	0.12637	11.131	0.022262	0.61567	0.027533	0.037782
LA (Boothalingam 2018)	5.4155	0.10687	0.18861	15.867	0.031734	0.878	0.039265	0.053309
LA-RE (Shaswat, personal communication)	3.8317	0.080861	0.12655	11.102	0.022204	0.61855	0.027663	0.037754
LU-SLnO	3.1713	0.070611	0.10305	9.1565	0.018313	0.5117	0.022884	0.031335
Learning percentage=60								
SLnO (Masadeh et al. 2019)	2.6478	0.058483	0.072587	6.3861	0.015965	0.39263	0.019632	0.026387
DA (Jafari and Chaleshtari 2017)	2.385	0.05425	0.065655	5.7561	0.01439	0.36013	0.018007	0.023744
LA (Boothalingam 2018)	3.9331	0.084856	0.10884	9.4354	0.023588	0.58537	0.029268	0.039038
LA-RE (Shaswat, personal communication)	2.0327	0.046695	0.054982	4.8547	0.012137	0.30325	0.015163	0.020248
LU-SLnO	1.9945	0.042507	0.053727	4.7481	0.01187	0.29456	0.014728	0.01987
Learning percentage=70								
SLnO (Masadeh et al. 2019)	2.3837	0.052789	0.050066	4.2531	0.014177	0.30619	0.017678	0.023715
DA (Jafari and Chaleshtari 2017)	2.4025	0.052118	0.050203	4.2655	0.014218	0.31053	0.017929	0.023867
LA (Boothalingam 2018)	2.2924	0.049382	0.047733	4.057	0.013523	0.29341	0.01694	0.022817
LA-RE (Shaswat, personal communication)	2.2268	0.047571	0.046757	3.9733	0.013244	0.28703	0.016572	0.022156
LU-SLnO	1.9343	0.04081	0.0405	3.4376	0.011459	0.24722	0.014273	0.019247
Learning percentage=80								
SLnO (Masadeh et al. 2019)	2.1668	0.041341	0.029938	2.5702	0.012851	0.22671	0.016031	0.021612
DA (Jafari and Chaleshtari 2017)	1.7731	0.032127	0.024232	2.0863	0.010432	0.18104	0.012801	0.017676
LA (Boothalingam 2018)	1.7282	0.037862	0.023713	2.0394	0.010197	0.17842	0.012616	0.017222
LA-RE (Shaswat, personal communication)	1.5315	0.026866	0.020975	1.8063	0.009032	0.15666	0.011077	0.015277
LU-SLnO	1.4701	0.024769	0.020219	1.7402	0.008701	0.15054	0.010645	0.014653

models and as the iteration gets increased, the error gets linearly decreased. At the 25th iteration, the proposed model remains with less error than in the range of ~ 8.5. Moreover, almost in all the iterations, the implemented approach is seemed to achieve better performance with minimum error in all the learning percentages.

For learning percentage 50, the proposed model in the 5th iteration has achieved the least error than DA and LA by 9.73% and 4.47%, respectively. Similarly, for the 25th iteration, the proposed work is 26.63%, 29.96%, 31.42%, and 14.83% better from SLnO, DA, LA, and LA-RE, respectively, with the minimized error. The analysis is also made for all other learning percentages and the resultants are graphically illustrated, where the proposed model shows its betterment over other conventional models.

Overall error analysis

Table 2 manifests the overall error analysis of the implemented approach over other classical approaches with respect to diverse learning percentages. In learning percentage 50, the proposed work regarding MD measure is achieved better with least value, which is 31.23%, 17.26%, 41.44%, and 17.24% improved than SLnO, DA, LA, and LA-RE, respectively. In the view of the RMSE measure, the proposed work achieves minimum RMSE error than other conventional models like SLnO, DA, LA, and LA-RE by 31.02%, 16.89%, 41.72%, and 17.28%, respectively. Subsequently, on considering learning percentage 80, the proposed model in response to MASE measure has attained betterment with minimized error, which is 32.46%, 16.56%, 14.73%, and 3.6% better from SLnO, DA, LA, and LA-RE, respectively. Similarly, all the other learning percentages are analyzed for all the error measures and are plotted in the table given below. The resultant outcomes thus explicated that the implemented approach has achieved better performance with less error than the existing approaches, thereby validates the betterment of implemented work with increased prediction accuracy.

Conclusions

The main intention of this implemented approach was on finding the reasonable applicability of optimized CNN for slump prediction in HSC. The input that applied for the following process was super-plasticizer, slag, cement, coarse

aggregate, water, fine aggregate, and fly ash. The prediction was made precise by incorporating the optimization logic in CNN by fine-tuning the filter size of the convolutional layer. This optimization was exploited by incorporating the two optimization algorithm concept and stated as LU-SLnO. The performance regarding the proposed work was evaluated and the results were compared over the traditional models in the view of convergence analysis and error measure. On considering convergence analysis, for learning percentage 50, the proposed model in the 5th iteration has achieved the least error than DA and LA by 9.73% and 4.47%, respectively. Similarly, for the 25th iteration, the proposed work is 26.63%, 29.96%, 31.42%, and 14.83% better from SLnO, DA, LA, and LA-RE, respectively, with the minimized error. The experimental results are encouraging and they have shown significant performance in predicting the slump. However, to ensure the reliability of the slump prediction, it is essential to experiment under diverse practical constraints and large datasets. Moreover, the real-time environment has to be simulated to the most possible extent. Our future research has been planned to accomplish diverse experimental platform and precise slump prediction model.

Availability of data and materials The dataset used for this paper is downloaded from the link: https://archive.ics.uci.edu/ml/datasets/Concrete+Slump+Test.

Authors' contributions Kumar Shaswat contributed to the design and implementation of the research, to the analysis of the results, and to the writing of the manuscript.

Compliance with ethical standards

Conflict of interest The authors declare that they have no conflict of interest.

Ethical approval The conducted research is not related to either human or animal use.

Consent to participate Not applicable.

Consent to publish Not applicable.

References

Abdalla LB, Ghafor K, Mohammed A (2019) Testing and modeling the young age compressive strength for high workability concrete modified with PCE polymers. Results in Materials:1

Agrawal V, Sharma A (2010) Prediction of slump in concrete using artificial neural networks. International Journal of Civil and Environmental Engineering 4(9)

Agudelo, Isabel (2009) Supply chain management in the cement industry. PhD diss, Massachusetts Institute of Technology

Amlashi AT, Abdollahi SM, Goodarzi S, Ghanizadeh AR (2019) Soft computing based formulations for slump, compressive strength, and elastic modulus of bentonite plastic concrete. J Clean Prod 230: 1197–1216

Bayar G, Bilir T (2019) A novel study for the estimation of crack propagation in concrete using machine learning algorithms. Constr Build Mater 215:670–685

Beno MM, Valarmathi IR, Swamy SM, Rajakumar BR (2014) Threshold prediction for segmenting tumour from brain MRI scans. Int J Imaging Syst Technol 24(2):129–137

Bondar D, Ma Q, Soutsos M, Basheer M, Nanukuttan S (2018) Alkali activated slag concretes designed for a desired slump, strength and chloride diffusivity. Constr Build Mater 190:191–199

Boothalingam R (2018) Optimization using lion algorithm: a biological inspiration from lion's social behavior. Evol Intel 11(1–2):31–52

Brammya, Deepa TA (2019) Job scheduling in cloud environment using lion algorithm. Journal of Networking and Communication Systems 2(1):1–14

Chandwani V, Agrawal V, Nagar R (2015) Modeling slump of ready mix concrete using genetic algorithms assisted training of artificial neural networks. Expert Syst Appl 42(21):885–893

Chen L, Kou C-H, Ma S-W (2014) Prediction of slump flow of high-performance concrete via parallel hyper-cubic gene-expression programming. Eng Appl Artif Intell 34:66–74

Domone P (1998) The slump flow test for high-workability concrete. Cem Concr Res 28(2):177–182

Fang G, Ho WK, Tu W, Zhang M (2018) Workability and mechanical properties of alkali-activated fly ash-slag concrete cured at ambient temperature. Constr Build Mater 172:476–487

Feng D-C, Liu Z-T, Wang X-D, Chen Y, Jiang Z-M (2020) Machine learning-based compressive strength prediction for concrete: an adaptive boosting approach. Construction and Building Materials: 230

Honglei C, Zuquan J, Tiejun Z, Benzhen W, Jian L (2020) Capillary suction induced water absorption and chloride transport in non-saturated concrete: the influence of humidity, mineral admixtures and sulfate ions. Construction and Building Materials:236

Jadhav AN, Gomathi N (2019) DIGWO: hybridization of dragonfly algorithm with improved grey wolf optimization algorithm for data clustering. Multimedia Research 2(3):1–11

Jafari M, Chaleshtari MHB (2017) Using dragonfly algorithm for optimization of orthotropic infinite plates with a quasi-triangular cut-out. European Journal of Mechanics A/Solids 66:1–14

Kaufmann J (2020) Evaluation of the combination of desert sand and calcium sulfoaluminate cement for the production of concrete. Constr Build Mater 243:118281

Li C, Miao L, You Q, Hu S, Fang H (2018) Effects of viscosity modifying admixture (VMA) on workability and compressive strength of structural EPS concrete. Constr Build Mater 175:342–350

Lu C, Yang H, Mei G (2015) Relationship between slump flow and rheological properties of self compacting concrete with silica fume and its permeability. Constr Build Mater 75:157–162

Ma K, Feng J, Long G, Xie Y, Chen X (2017) Improved mix design method of self-compacting concrete based on coarse aggregate average diameter and slump flow. Constr Build Mater 143:566–573

Masadeh R, Mahafzah B, Sharieh A (2019) Sea lion optimization algorithm. International Journal of Advanced Computer Science and Applications 10:388–395

Meng W, Kumar A, Khayat KH (2019) Effect of silica fume and slump-retaining polycarboxylate-based dispersant on the development of properties of Portland cement paste. Cem Concr Compos 99:181–190

Nair AT, Muthuvel K (2019) Diabetic retinopathy recognition using enhanced crow search with levy flight algorithm. Multimedia Research 2(4):43–52

Nguyen NT, Yu Y, Li J, Gowripalan N, Sirivivatnanon V (2019) Elastic modulus of ASR-affected concrete: an evaluation using artificial neural network. Comput Concr 24(6):541–553

Nguyen TN, Yu Y, Li J, Sirivivatnanon V (2020) An optimised support vector machine model for elastic modulus prediction of concrete subject to alkali silica reaction. In: ACMSM25. Springer, Singapore, pp 899–909

Nilsen V, Pham LT, Hibbard M, Klager A, Morgan D (2019) Prediction of concrete coefficient of thermal expansion and other properties using machine learning. Constr Build Mater 220:587–595

O'Shea K, Nash R (2015) An introduction to convolutional neural networks. ArXive-prints

Prasad M, Huang C-J, Song X-B, Chen S-J, Qian C-H (2020) Concrete behavior in steel-concrete-steel panels subjected to biaxial tension compression. Journal of Constructional Steel Research:167

Rousseau MAD, Laftchiev E, Kasprzyk JR, Rajagopalan B, Srubar WV (2019) A comparison of machine learning methods for predicting the compressive strength of field-placed concrete. Construction and Building Materials:228

Shafiq N, Choo CS, Isa MH (2018) Effects of used engine oil on slump, compressive strength and oxygen permeability of normal and blended cement concrete. Constr Build Mater 187:178–184

Sokhansefat G, Ley MT, Cook MD, Alturki R, Moradian M (2019) Investigation of concrete workability through characterization of aggregate gradation in hardened concrete using X-ray computed tomography. Cem Concr Compos 98:150–161

Taghipour, Atour, Frayret J-M (2013) Coordination of operations planning in supply chains: a review. International Journal of Business Performance and Supply Chain Modelling 5(3):272–307

Tay YWD, Qian Y, Tan MJ (2019) Printability region for 3D concrete printing using slump and slump flow test. Engineering, Composites Part B, p 174

Vieira LBP, Figueiredo AD (2020) Implementation of the use of hydration stabilizer admixtures at a ready-mix concrete plant. Case Studies in Construction Materials 12

Vosooghidizaji M, Taghipour A, Canel-Depitre B (2020) Supply chain coordination under information asymmetry: a review. Int J Prod Res 58(6):1805–1834

Yeh I (2008) Modeling slump of concrete with fly ash and superplasticizer. Comput Concr 5(6):559–572

Yeh, I-Cheng (2006) Exploring concrete slump model using artificial neural networks. J Comput Civ Eng 20(3):217–221

Yeh, I-Cheng (2007) Modeling slump flow of concrete using second-order regressions and artificial neural networks. Cem Concr Compos 29(6):474–480

Yeh, I-Cheng (2008) Prediction of workability of concrete using design of experiments for mixtures. Comput Concr 5(1):1–20

Yeh, I-Cheng (2009) Simulation of concrete slump using neural networks. Constr Mater 162(1):11–18

Yu Y, Li W, Li J, Nguyen TN (2018) A novel optimised self-learning method for compressive strength prediction of high performance concrete. Constr Build Mater 184:229–247

Yu Y, Zhang C, Gu X, Cui Y (2019) Expansion prediction of alkali aggregate reactivity-affected concrete structures using a hybrid soft computing method. Neural Comput & Applic 31(12):8641–8660

Yuan T-F, Lee J-Y, Yoon Y-S (2020) Enhancing the tensile capacity of no-slump high-strength high-ductility concrete. Cem Concr Compos 106:103458

Zheng L, Cheng H, Huo L, Song G (2019) Monitor concrete moisture level using percussion and machine learning. Constr Build Mater 229:117077